Progress In Electromagnetics Research, Vol. 163, 119–132, 2018

DROP Algorithm for Super Resolution Scattering Center Extraction

Young-Jae Choi and In-Sik Choi*

Abstract—The scattering center extraction algorithm is a method to estimate the scattering center from the backscattered field. Superior scattering center extraction algorithms should be robust to noise, independent of the model order, and automatically and quickly operated. In this paper, we propose a novel super resolution scattering center extraction algorithm that satisfies the conditions mentioned above, which has been named the dimension reduced optimization problem (DROP). Using DROP, we determined a one-dimensional scattering center from a high resolution range profile and a two-dimensional scattering center from an inverse synthetic aperture radar image.

1. INTRODUCTION

The radar cross section (RCS) is the ratio of the scattered power to the incident power in the farfield [1]. The RCS provides a great deal of information about a target [2]. The scattering center is the point that radiates the highest energy on the target, and information about it can be obtained from the RCS. The scattering center is mainly used for target detection and target recognition. It is important to extract the scattering center from the backscattered field. A scattering center extraction algorithm is the method used to discern the parameters of the scattering center, such as range, amplitude, and phase from the backscattered field. The basic strategy for extracting scattering centers is to use the inverse fast Fourier transform (IFFT) algorithm. It is widely used in many applications due to its fast operation and robustness to noise. However, there is a resolution limitation caused by the IFFT bin size.

To overcome this limitation, many super resolution algorithms have been developed. There are two main strategies to these algorithms. First are model based methods, such as Prony's method, matrix pencil (MP), estimation of signal parameters via rotational invariance techniques (ESPRIT), generalized eigenvalues utilizing signal subspace eigenvectors (GEESE), and multiple signal classification (MUSIC) [3–9]. Model-based methods can be computed quickly and have high resolutions, but are sensitive to noise and require the initial value estimation or model order estimation. Unfortunately, it is difficult to determine model order estimation and initial value estimation for targets with complex shapes.

The other method is to use optimization techniques for extraction of scattering centers. Li et al. [10] proposed the scattering center extraction method using a genetic algorithm. This method overcame the limitations of model based methods. It is completely automatic, robust to noise, and does not require initial value estimation or model order estimation. However, its computation time is very long because it must optimize all parameters of all scattering centers on the target [10]. To overcome this problem, Choi and Kim proposed the evolutionary programming (EP)-based CLEAN algorithm, improving computational performance [11–13]. The EP-based CLEAN reduces the required dimensions of the scattering center extraction by employing the CLEAN algorithm [14]. This procedure allows one scattering center to be extracted at a time instead of all scattering centers at once. However,

Received 23 August 2018, Accepted 5 October 2018, Scheduled 7 November 2018
* Corresponding author: In-Sik Choi (recog@hnu.kr).
The authors are with the Department of Electronic Engineering, Hannam University, Daejeon 34430, Korea.

EP-based CLEAN must solve a three-dimensional optimization problem regarding range, amplitude, and phase [11], which requires lengthy computation time to solve using stochastic search methods such as EP and particle swarm optimization [15]. There are two strategies to improve the computational performance of this optimization problem. One is to reduce the dimensions of the optimization problem. The other is to change the problem to a convex optimization problem. Because there is no local minimum in a convex optimization problem, it can be solved by quickly-operated algorithms, such as a backtracking line search method [16].

In previous research, we proposed an algorithm that applied these two strategies [17]. The method proposed in the article "A novel fast clean algorithm using the gradient descent method" can be operated more quickly than the EP-based CLEAN [17]. However, the phase of the scattering center had to be re-optimized at each iteration of the range optimization process, which required too much computational time [17]. If this process can be solved by using least squares, the computational performance can be largely improved [18]. In this paper, we propose a new method to improve the previous one, and we expand the improved algorithm to the two-dimensional scattering center extraction method. To improve the method, we applied the direct solution of the complex least squares problem [17], and we have named the new proposed method as the dimension reduced optimization problem (DROP).

2. ONE DIMENSIONAL DROP ALGORITHM

2.1. Parameter Estimation of the Scattering Center

By the undamped exponential model, the backscattered field is given by

$$E_q = \sum_{m=1}^{M} a_m \exp\left[j\theta_m\right] \exp\left[-j4\pi f_q R_m/c\right] \tag{1}$$

where $q = 1, 2, \ldots, Q$; m is the index of scattering center; M is the number of scattering centers, $c = 3 \times 10^8$ (m/s) and is the velocity of light; R_m is the range of the mth scattering center; f_q is the sampling frequency; Q is the number of frequency samples; a_m is the amplitude of the mth scattering center; and θ_m is the phase of the mth scattering center [19]. Equation (1) can be represented by

$$\vec{E} = [E_1,\, E_2,\, E_q, \ldots,\, E_Q]^T \tag{2}$$

Scattering center extraction is used to estimate the parameters of the scattering center, such as amplitude, phase, and range. If the range of the scattering center is determined, the associated amplitude a and phase θ of the determined range R can be calculated by

$$\min_{a,\,\theta} \left\| \vec{E} - \vec{S} a \exp\left[j\theta\right] \right\| \tag{3}$$

where $\|\vec{x}\| = \sqrt{\sum_{k=1}^{K} |x_k|^2}$, $\vec{x} = [x_1,\, x_2,\, x_k, \ldots,\, x_K]^T$ and $\vec{S}$ is given by

$$\vec{S} = [s_1,\, s_2,\, s_q,\, \ldots,\, s_Q]^T \tag{4}$$

where $s_q = \exp[-j4\pi f_q R/c]$. The symbols a and θ from Eq. (3) can be calculated by the solution of a complex least squares problem with constrained phase [18]:

$$\theta = \frac{1}{2} \angle \left(\vec{S}^H \vec{E} \right)^T M^+ \left(\vec{S}^H \vec{E} \right) \tag{5}$$

$$a = M^+ \mathrm{Re}\left(\vec{S}^H \vec{E} \exp\left[-j\theta\right] \right) \tag{6}$$

where $M \equiv \mathrm{Re}(\vec{S}^H \vec{S})$ is a real part of $\vec{S}^H \vec{S}$, M^+ the pseudo inverse of M, and $\vec{S}^H$ the conjugate transpose of $\vec{S}$. The range of scattering center R can be calculated by

$$\min_{R} \left\| \vec{E} - \vec{S} \exp\left[j\theta_R\right] \right\| \tag{7}$$

where θ_R is the phase calculated by Eq. (3) depending on R. Because θ_R depends on R, it should be recalculated about R for each iteration. Thus, Eq. (7) should be calculated by the iterative method, where R_{init} is obtained by the peak search of the range profile of $\vec{E}$. All of the parameters for the single scattering center can be obtained by solving Eqs. (3) and (7) using the appropriate initial value of R. The component of the extracted scattering center can be cancelled from $\vec{E}$ by

$$\vec{E}_{\text{next}} = \vec{E} - a \exp[j\theta] \vec{S} \tag{8}$$

where $s_q = \exp[-j4\pi f_q R/c]$. If the scattering center requires further extraction, repeat Eqs. (3) to (8) after $\vec{E} = \vec{E}_{\text{next}}$.

2.2. Detailed Implementation of the One-Dimensional DROP Algorithm

The detailed algorithm is as follows:

(Step 1) Set $m = 1$ where m is an iterator index.

(Step 2) Set variables to initial value as shown in Table 1.

Table 1. Initial values setting in the one-dimensional DROP algorithm.

Variable	Initial Value	Description
R	R_{init}	initial range value of the scattering center about range profile of $\vec{E}_m$
ΔR	$\frac{c}{4BW}$	range interval where BW is bandwidth
$\vec{E}_m$	$\vec{E}$	scattered field

(Step 3) Calculate the parameters of the scattering center as shown in Table 2 where $s_q = \exp[-j4\pi f_q R/c]$.

Table 2. Calculate the parameters of the scattering center in the one-dimensional DROP algorithm.

Equation	K
$\theta_R = \min_{\theta} \|\vec{E}_m - \vec{S}a \exp[j\theta]\|$	R
$\theta_{R-\Delta R} = \min_{\theta} \|\vec{E}_m - \vec{S}a \exp[j\theta]\|$	$R - \Delta R$
$\theta_{R+\Delta R} = \min_{\theta} \|\vec{E}_m - \vec{S}a \exp[j\theta]\|$	$R + \Delta R$
$J_R = \|\vec{E}_m - \vec{S} \exp[j\theta_R]\|$	R
$J_{R-\Delta R} = \|\vec{E}_m - \vec{S} \exp[j\theta_{R-\Delta R}]\|$	$R - \Delta R$
$J_{R+\Delta R} = \|\vec{E}_m - \vec{S} \exp[j\theta_{R+\Delta R}]\|$	$R + \Delta R$

(Step 4) Repeat the operation for Table 3.

(Step 5) Substitute $R_m = R$ and calculate a_m and θ_m using Eqs. (5) and (6) where $s_q = \exp[-j4\pi f_q R_m/c]$.

(Step 6) Obtain $\vec{E}_{m+1}$ using Eq. (8). If m is the number of scattering centers, terminate algorithm; otherwise, jump to step 2 after setting $m = m + 1$.

Table 3. Loop control condition in the one-dimensional DROP algorithm.

Condition	Action	Next Step
$J_R < J_{R+\Delta R}$ & $J_R < J_{R-\Delta R}$	$\Delta R = \Delta R/2$	Step 3
$J_R > J_{R+\Delta R}$	$R = R + \Delta R$	Step 3
$J_R > J_{R-\Delta R}$	$R = R - \Delta R$	Step 3
$\Delta R < 10^{-4}$	Termination	Step 5

3. TWO DIMENSIONAL DROP ALGORITHM

3.1. Parameter Estimation of the Scattering Center

By the undamped exponential model, the two-dimensional backscattered field is given by

$$E_{p,q} = \sum_{m=1}^{M} a_m \exp\left[j\theta_m\right] \exp\left[-j4\pi \vec{D}_{p,q}\, \vec{K}_m/c\right] \tag{9}$$

where $\vec{D}_{p,q} = [\ f_q \cos(\Phi_p) \quad f_q \sin(\Phi_p)\ ]$, $q = 1, 2, \ldots, Q$, $p = 1, 2, \ldots, P$, and $\vec{K}_m = [\ X_m \quad Y_m\ ]^T$ (the other parameters are shown in Table 4) [19]. Equation (9) can be represented by

$$\mathrm{E} = [E_{p,q}] \tag{10}$$

where E is $P \times Q$ matrix. If X and Y are determined, the associated amplitude a and phase θ can be calculated by

$$\min_{a,\,\theta} \|\mathbf{E} - \mathbf{S} a \exp\left[j\theta\right]\| \tag{11}$$

where $\|\mathbf{x}\| = \sqrt{\sum_{p=1}^{P}\sum_{q=1}^{Q} |x_{p,\,q}|^2}$, $\mathbf{x} = [x_{p,q}]$ is a $P \times Q$ matrix, and $\mathbf{S}$ is given by

$$\mathbf{S} = [s_{p,q}] \tag{12}$$

where $s_{p,q} = \exp[-j4\pi \vec{D}_{p,q} \vec{K}/c]$, $\vec{K} = [\ X \quad Y\ ]^T$, $\mathbf{S}$ is $P \times Q$ matrix, and a and θ of Eq. (11) can be calculated by [18]

$$\theta = \frac{1}{2} \angle \left(\vec{S}^H \vec{E}\right)^T M^+ \left(\vec{S}^H \vec{E}\right) \tag{13}$$

$$a = M^+ \mathrm{Re}\left(\vec{S}^H \vec{E} \exp\left[-j\theta\right]\right) \tag{14}$$

where $\vec{S} = [\ s_{1,1\ldots Q} \quad s_{2,1\ldots Q} \quad s_{p,1\ldots Q} \quad \ldots \quad s_{P,1\ldots Q}\ ]^T$ and $\vec{E} = [\ E_{1,1\ldots Q} \quad E_{2,1\ldots Q} \quad E_{p,1\ldots Q} \quad \ldots \quad E_{P,1\ldots Q}\ ]^T$.

Table 4. Parameters of the two-dimensional backscattered field.

Symbol	Description
P	number of the frequency sampling
Q	number of the angle sampling
X_m, Y_m	location of mth scattering center
f_q	qth sampled frequency
f_c	center frequency
Φ_p	pth sampled angle

The position of the scattering center $\vec{K}$ can be calculated by

$$\min_{X,Y} \|\mathbf{E} - \mathbf{S}a_K \exp[j\theta_K]\| \tag{15}$$

where a_K and θ_K are amplitude and phase calculated by Eq. (11) about $\vec{K}$, and the initial vector of $\vec{K}$ is obtained by searching the minimum point of the cost space image about $\mathbf{E}$. Because θ_K depends on $\vec{K}$, it should be recalculated about $\vec{K}$ of each iteration. Thus, Eq. (15) should be calculated by the iterative method. The component of the extracted scattering center can be cancelled from $\mathbf{E}$ by

$$\mathbf{E}_{\text{next}} = \mathbf{E} - ae^{j\theta}\mathbf{S} \tag{16}$$

where $s_{p,q} = \exp[-j4\pi\vec{D}_{p,q}\vec{K}/c]$. If the scattering center requires further extraction, repeat Eqs. (11) to (16) after $\mathbf{E} = \mathbf{E}_{\text{next}}$.

3.2. Detailed Algorithm

The detailed algorithm is as follows:

(Step 1) Set $m = 1$ where m is the iteration index.

(Step 2) Set variables to initial value as shown in Table 5.

Table 5. Initial values setting in the two-dimensional DROP algorithm.

Variable	Initial Value	Description
$\vec{L}$	$[\ X \quad Y\ ]^T$	initial location of the scattering center of $\mathbf{E}_m$
ΔL	$\frac{c}{4BW}$	location interval
∇J_L	$[\ \frac{\partial J}{\partial X} \quad \frac{\partial J}{\partial Y}\ ]^T$	gradient of the cost function J_L
$\mathbf{E}_m$	$\mathbf{E}$	scattered field

(Step 3) Calculate Table 6 where $s_{p,q} = \exp[-j4\pi\,\vec{D}_{p,q}\vec{K}/c]$.

Table 6. Calculate the parameter of the scattering center in the two-dimensional DROP algorithm.

Equation	$\vec{K}$
$a_L,\ \theta_L = \min_{a,\,\theta} \|\mathbf{E} - \mathbf{S}a\exp[j\theta]\|$	$\vec{L}$
$J_L = \|\mathbf{E} - \mathbf{S}a_L\exp[j\theta_L]\|$	$\vec{L}$
$\nabla J_L = [\ \frac{\partial J_L}{\partial X} \quad \frac{\partial J_L}{\partial Y}\ ]^T$	$\vec{L}$
$a_\Delta,\ \theta_\Delta = \min_{a,\,\theta} \|\mathbf{E} - \mathbf{S}a\exp[j\theta]\|$	$\vec{L} - \frac{\nabla J_L}{\|\nabla J_L\|}\Delta L$
$J_\Delta = \|\mathbf{E} - \mathbf{S}a_\Delta\exp[j\theta_\Delta]\|$	$\vec{L} - \frac{\nabla J_L}{\|\nabla J_L\|}\Delta L$

(Step 4) Repeat the operation for Table 7.

(Step 5) Substitute $\vec{K}_m = \vec{L}$ and calculate a_m and θ_m solving $\min_{a_m,\,\theta_m} \|\mathbf{E}_m - \mathbf{S}a_m\exp[j\theta_m]\|$ where $s_{p,q} = \exp[-j4\pi\vec{D}_{p,q}\vec{K}_m/c]$.

(Step 6) Obtain $\mathbf{E}_{m+1}$ using Eq. (16). If m is the number of scattering centers, terminate algorithm; otherwise, jump to Step 2 after setting $m = m + 1$.

Table 7. Loop control condition in the two-dimensional DROP algorithm.

Condition	Action	Next Step
$J_L \leq J_{\Delta L}$	$\Delta L = \frac{\Delta L}{2}$	Step 3
$J_L > J_{\Delta L}$	$\vec{L} = \vec{L} - \frac{\nabla J_L}{\|\nabla J_L\|}\Delta L$	Step 3
$\Delta L < 10^{-4}$	Termination	Step 5

3.3. Initial Value of the Two-Dimensional DROP

In the one-dimensional DROP, the highest value of the range profile was used to the initial value of the scattering center. In the two-dimensional DROP, we can expect to use the same operation as the one-dimensional DROP by determining the highest value of the ISAR image as the initial value. Unfortunately, this often causes failed extraction of the scattering center because the highest location in the ISAR image is not always the same as the location of the scattering center. For this reason, we should obtain the image of the cost function space, and we should use the lowest location as the initial value. The image of the cost function space can be obtained by

$$\mathbf{V} = [v_{p,q}] \tag{17}$$

where $v_{p,q} = \left\| \mathbf{E} - \mathbf{S}a_{\vec{K}_{p,q}} e^{j\theta_{\vec{K}_{p,q}}} \right\|$, $\vec{K}_{p,q} = [\ X_q \quad Y_p\ ]^T$, and $\mathbf{V}$ is $P \times Q$ matrix. The range resolution and cross-range resolution should be determined in the same way as the ISAR image [19].

The two-dimensional DROP is a very stable operation when we use the lowest location of the cost function space as the initial value. But it requires too much computational work to calculate the cost function space. Although it is not accurate, the scattering center is located near the highest location in the ISAR image. Therefore, we can reduce the computation time by calculating only the cost function space which is near the highest position in the ISAR image. In Fig. 1, the highest location in the ISAR image and the location of the scattering center are different. However, the 7×7 image of cost function, which is near the highest location in the ISAR image, includes the lowest location of the cost function space. The computational resolution of the cost function space should be determined to be equal to the resolution of the ISAR image.

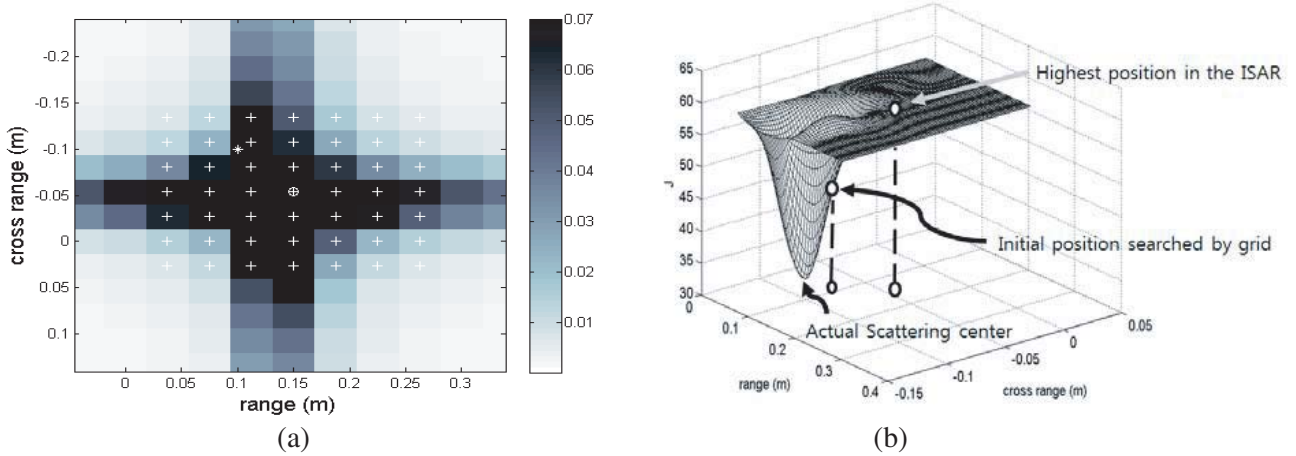

(a) (b)

Figure 1. Cost function space for determining the initial value of the 2D DROP. (a) IFFT-based ISAR, grid for cost function space, and position of scattering center where $*$ is the position of the actual scattering center, $+$ is the calculation point for cost function space, and o is the highest position in the IFFT-based ISAR. (b) The cost function space near the highest location in the ISAR image; frequency: $8.3 \sim 12.3$ GHz; aspect angle: $-6.8698 \sim 6.8698°$; $X = 0.1$ m, $Y = -0.1$ m; the number of frequency sampling: 41; the number of angle sampling: 57.

4. CONVERGENCE ISSUE

DROP algorithm solves optimization problem to estimate parameters of scattering center. It requires long computation time to solve optimization problem. Three tricks are employed to DROP algorithm for reducing computation time. The first trick is a CLEAN procedure. The CLEAN procedure converts the complex problem in which parameters of all scattering center should be estimated at once, to the simple problem in which parameters of only one scattering center should be estimated at the each iteration. To apply CLEAN procedure, we had to assume that components of all scattering centers are orthogonal.

The second trick is an initial value selection for the optimization. Since these cost function spaces contain many local minima, we cannot use fast optimization technique such as gradient descent. To overcome the local minimum problem, EP-based CLEAN uses stochastic search method which requires much computation time. Fig. 2 shows the relation between cost function space and range profile. The peak point of range profile always exists in concave region of cost function. There are no local minima in concave region. Thus, DROP algorithm is always converged by the solution of convex optimization such as gradient descent, if the peak point of range profile is determined as the initial value of R. Two dimensional DROP is also always converged, if the initial value is in the concave region. However, the peak point of the ISAR image is not always located in the concave region of the cost function space because the peak point of the ISAR image depends on the imaging algorithm. For this reason, we use IFFT and grid of cost function to search the initial value that is in the concave region of the cost function.

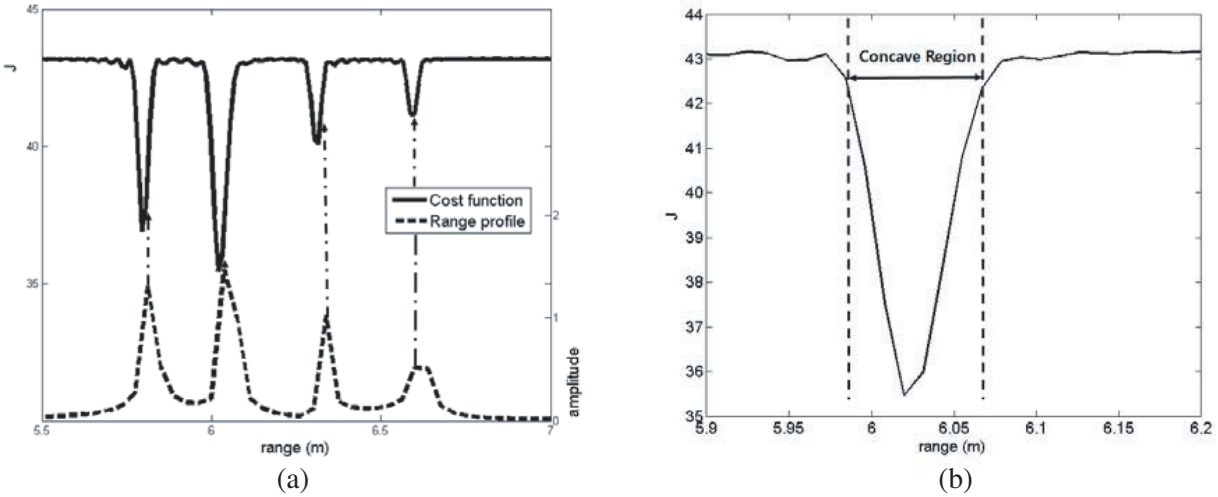

Figure 2. Cost function space of one dimensional DROP: (a) relation between range profile and cost function space; (b) concave region of cost function.

The third trick is that the dimension of the optimization problem to extract scattering center was reduced. The EP-based CLEAN should obtain three parameters such as real part of amplitude, imaginary part of amplitude, and range of scattering center at once by solving three dimensional optimization problem. However, we found that the optimization problem about range and the optimization problem about amplitude and phase can be separated, and the optimization problem about amplitude and phase can be simply solved by the solution of a complex least squares problem with constrained phase [18]. Thus three dimensional optimization of EP-based CLEAN can be converted to one dimensional optimization DROP algorithm. Moreover, the optimization problem of DROP algorithm can be fast solved by the solution of convex optimization such as gradient descent because that is free of a local minimum problem.

As a result, the convergence of the DROP algorithm depends on the initial value. If there is the initial value in the concave region, DROP algorithm is always converged. In the case of one dimensional

DROP, the resolution of the one Fourier bin in range profile and the width of concave region in cost function space are same as $c/2B$. Therefore, one dimensional DROP is always converged. On the other hand, the shape and position of the one Fourier bin in ISAR image is not matched with the concave region of cost function space. Thus, the two-dimensional DROP must determine the initial value more carefully.

5. SIMULATION

5.1. The One-Dimensional DROP

To evaluate the performance of the one-dimensional DROP, we compared the results from DROP with the previously published method [17]. These simulations were performed using an Intel® Core™ i7-4790 CPU 3.60 GHz processor and three types of data: synthetic, numerical, and measured.

The first case was the synthetic data. It was generated by the ideal point scatter model of Eq. (1). The sampled frequency was from 8.3 GHz to 12.3 GHz at 256 points. Table 8 shows the parameters of the scattering centers (amplitude, range, and phase). In Table 8, although the range resolution of the synthetic data is 0.0375 m, the interval between the second scattering center and third scattering center was 0.025 m. Fig. 3 shows the scattering centers extracted by DROP and the previously-published method [17]. Also, Fig. 2 shows the relative error (RE) between the original field and reconstructed field following the signal to noise ratio (SNR). RE is calculated by

$$\mathrm{RE} = \frac{\left\| \vec{E}^{\mathrm{actual}} - \vec{E}^{\mathrm{recon}} \right\|}{\left\| \vec{E}^{\mathrm{actual}} \right\|} \tag{18}$$

Table 8. Parameters of the synthetic data for simulation of the one-dimensional scattering center extraction.

m	Amplitude	Range (m)	Phase (Radian)
1	1.5	5.8	2
2	1.5	6.0150	0.9
3	1.2	6.0400	0.7854
4	1	6.3073	0
5	0.8	6.5939	0.9151

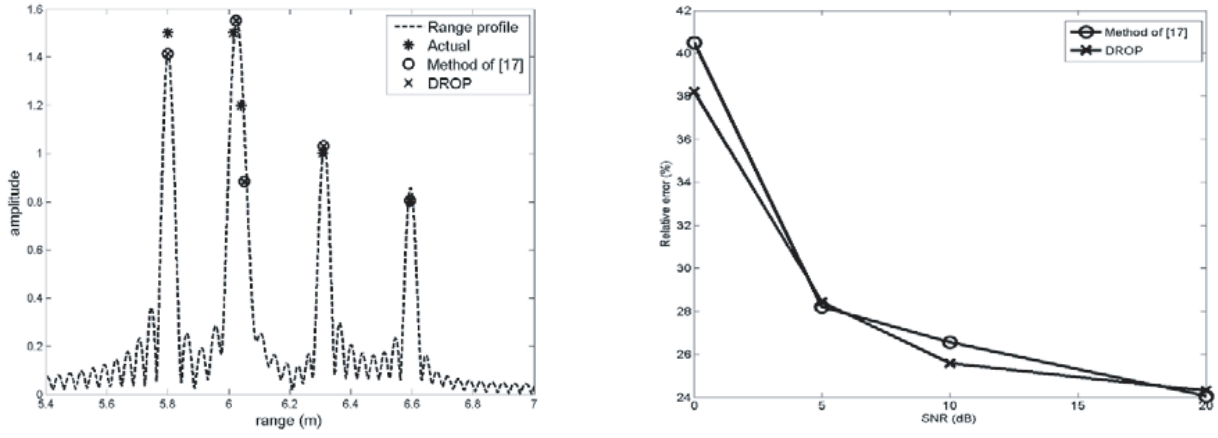

(a) (b)

Figure 3. Simulation results for the synthetic data: (a) range profile and extracted scattering centers; (b) RE according to SNR.

where $\|\vec{x}\| = \sqrt{\sum_{k=1}^{K} |x_k|^2}$, $\vec{E}^{\text{actual}}$ is the actual backscattered field, and $\vec{E}^{\text{recon}}$ is a reconstructed backscattered field by extracted scattering centers. Since the one-dimensional DROP is an algorithm to improve upon the computation time of the previously-published method [17], the scattering center extracted by DROP should be the same as that of the previous method [17]; the result shown in Fig. 2 is what we expected. The computation time of DROP was about 0.03 second, and that of the previous method was about 0.23 second [17]. Thus, the computation time of DROP was about 7.6 times faster than the previous method [17].

The second case was the numerical data. We used a 1 : 16 scaled 3D computer aided design (CAD) model of an F-15 aircraft. The numerical data were calculated using physical optics. The sampling frequency was from 8.3 GHz to 12.3 GHz at 41 points. The azimuth angle and elevation angle were 0°. The five scattering centers were extracted. Fig. 4 shows the results of the simulation for the numerical data. The computation time of DROP was about 0.027 seconds, and that of the previous method was

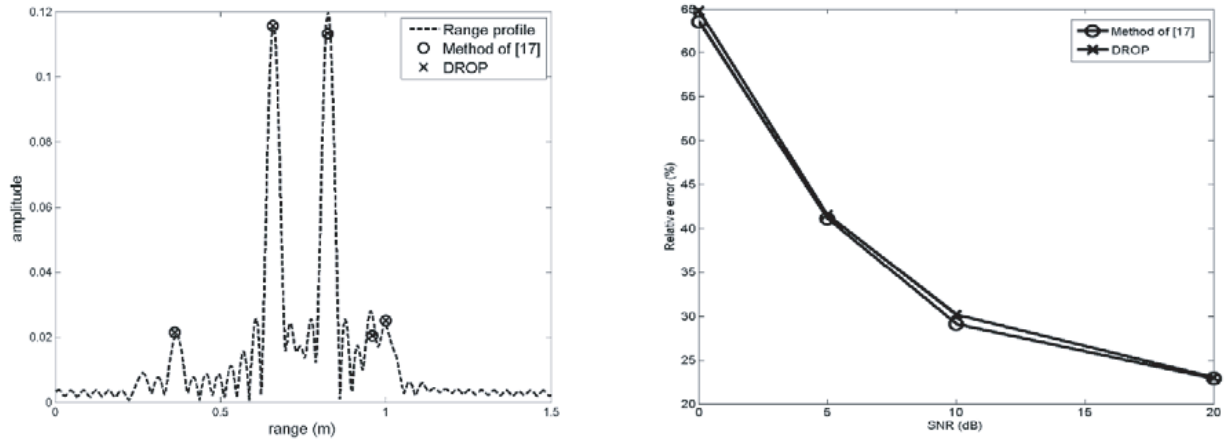

(a) (b)

Figure 4. Simulation result for the numerical data: (a) range profile and extracted scattering centers; (b) RE according to SNR.

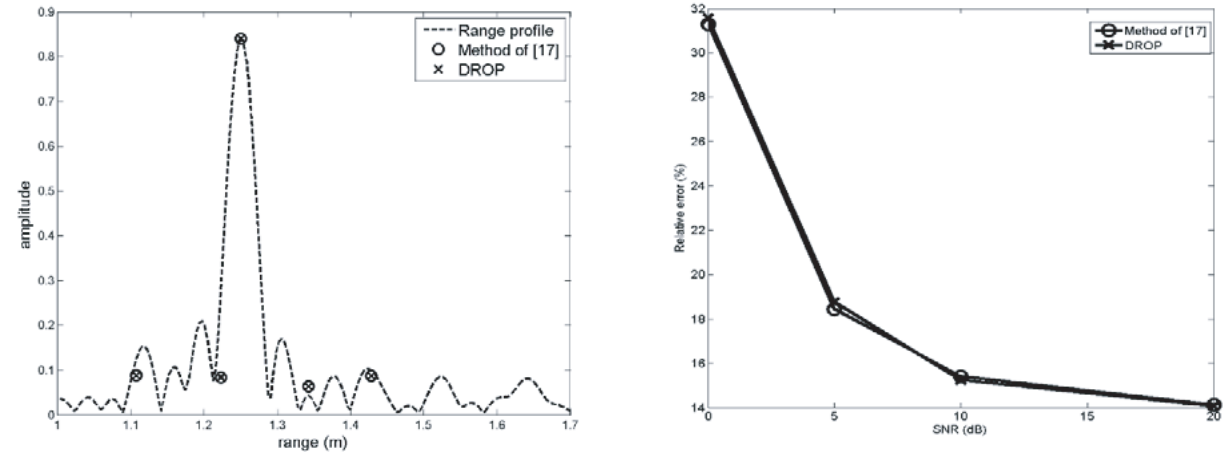

(a) (b)

Figure 5. Simulation result for the measured data: (a) range profile and extracted scattering centers; (b) RE according to SNR.

about 0.081 seconds [17]. Thus, the computation time of DROP was about 3 times faster than the previous method [17].

The third case was measured data. The target was the 1 : 16 scaled model of the F-14 Tomcat. The RCS of the target was measured using the compact range at the Pohang University of Science and Technology (POSTECH). The measurement frequency was 8.3 to 12.3 GHz with 401 sampling points. The azimuth and elevation angles were both 0° [20]. Five scattering centers were extracted. Fig. 5 shows the result of the simulation for the measured data. The computation time of DROP was about 0.037 seconds compared to 0.325 seconds for the previous method [17]. Thus, the computation time of DROP was about 8.7 times faster than the previous method [17].

5.2. Two-Dimensional DROP

To verify the performance of the two-dimensional DROP, we performed scattering center extraction for three types of data: synthetic, numerical, and measured. This simulation was performed using an Intel® Core™ i7-4790 CPU 3.60 GHz processor. In all of the simulations, the sampling frequency was 8.3 to 12.3 GHz; the aspect angle was −11.2 to 11.2°; the number of sampling frequencies (Q) was 41 points; and the number of sampling angles (P) was 57 points. The first case was synthetic data. The signal model was given by Eq. (9). The parameters of the scattering centers are shown in Table 9. Fig. 6 shows the ISAR image of the synthetic data and scattering center extracted by DROP. In this simulation, five scattering centers were extracted. The computation time of DROP was about 0.194 seconds, and that of the previous method was about 168.724 seconds [17]. Thus, the computation time of DROP was about 869 times faster than the previous method [17].

The second case was numerical data. The numerical method used physical optics. It was calculated by FEKO. The target was a 1 : 16 scale 3D CAD model of an F-15 aircraft. The 3D CAD model of the target and the ISAR image are shown in Fig. 7. In this simulation, 9 scattering centers were extracted.

Table 9. Parameters of the synthetic data for simulation with two-dimensional scattering centers.

m	Amplitude	Range (m)	Cross Range (m)	Phase (Radian)
1	1.5	−0.3333	0	2
2	1.4	0.1667	0.2333	0.9
3	1.3	0.1667	0	0.7854
4	1.4	0.1667	−0.2333	0
5	1.5	0.3333	0	0.9151

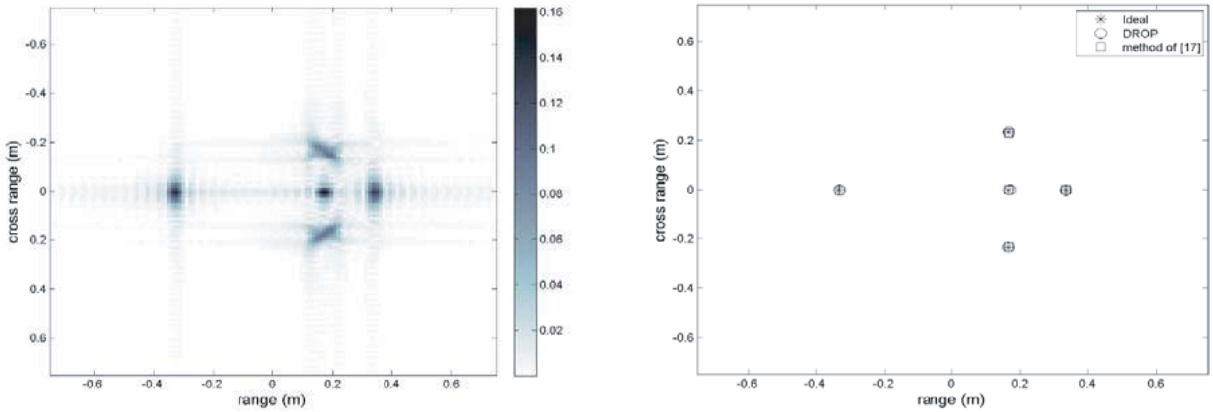

(a) (b)

Figure 6. Simulation result for the synthetic data: (a) ISAR image; (b) extracted scattering centers.

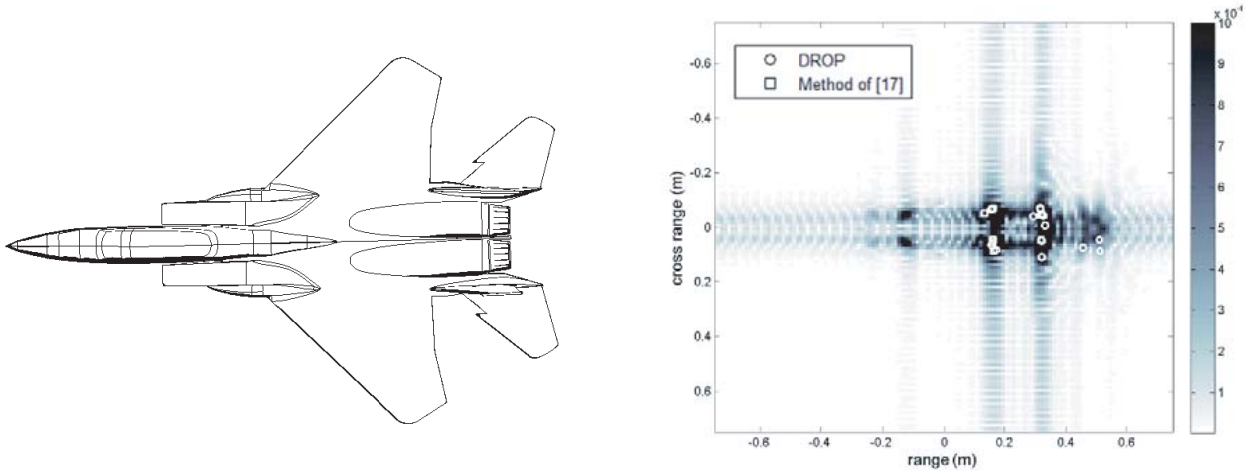

(a) (b)

Figure 7. Simulation result for the numerical data: (a) 3D CAD model; (b) ISAR image and extracted scattering centers.

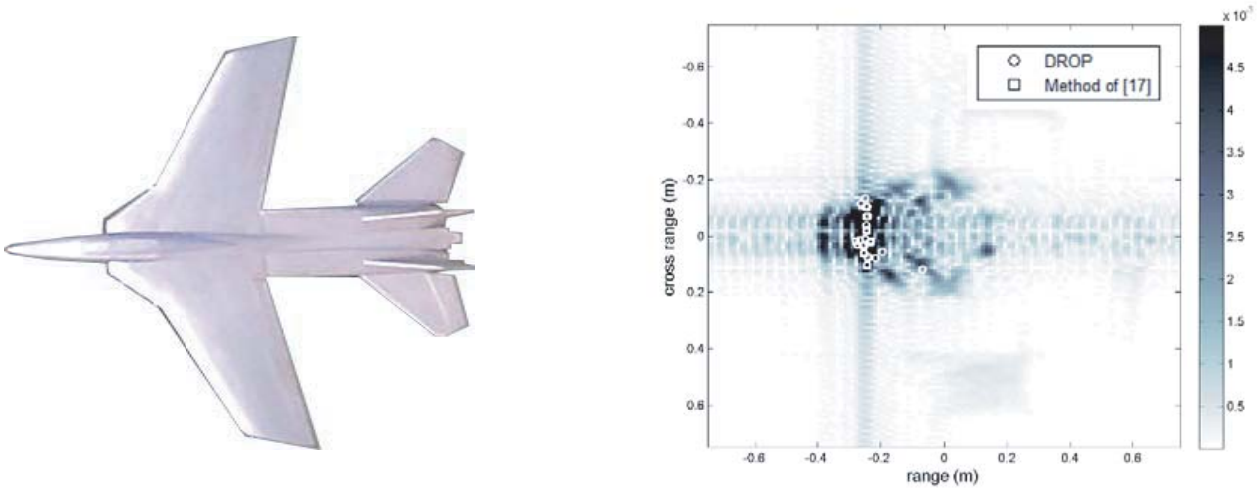

(a) (b)

Figure 8. Simulation result for the measured data: (a) 1 : 16 scaled model; (b) ISAR image and extracted scattering centers.

The computation time of DROP was about 3.032 seconds, and that of the previous method was about 159.449 seconds [17]. Thus, the computation time of DROP was about 52 times faster than the previous method [17].

The third case was measured data. The target was the 1 : 16 scale model of the F-14 Tomcat. It was measured using the compact range at the POSTECH [20]. The overview of the target and ISAR image are shown in Fig. 8. In this simulation, 9 scattering centers were extracted. The computation time of DROP was about 3.152 seconds compared to about 159.457 seconds for the previous method [17]. Thus, the computation time of DROP was about 50 times faster than the previous method [17].

Figure 9 shows the performance of the two-dimensional DROP in a noise environment. We performed 50 Monte Carlo simulations to determine the reliability of the results. RE is redefined by

$$\mathrm{RE} = \frac{\left\|\mathbf{E}^{\mathrm{actual}} - \mathbf{E}^{\mathrm{recon}}\right\|}{\left\|\mathbf{E}^{\mathrm{actual}}\right\|} \tag{19}$$

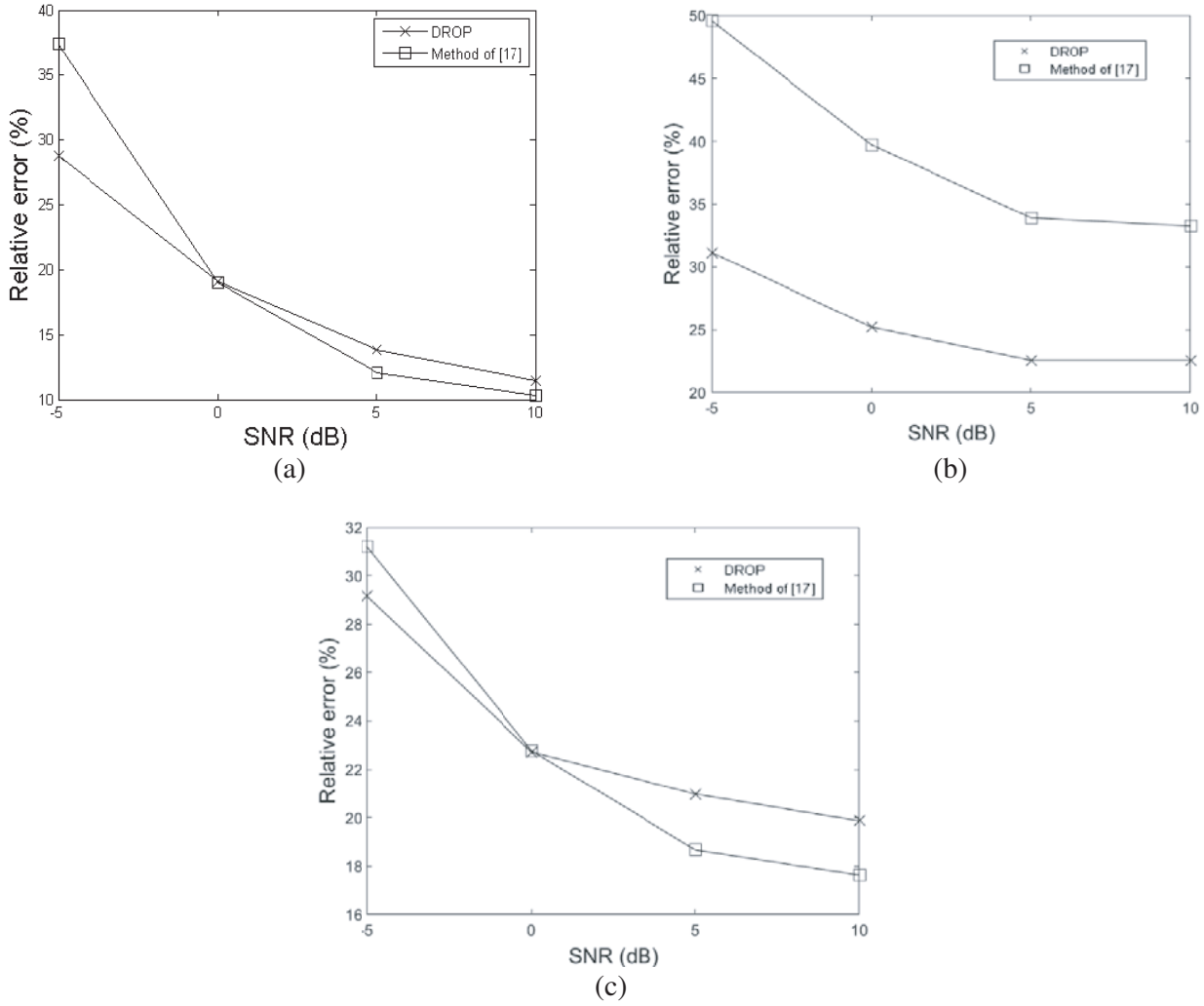

Figure 9. Result of noise simulation: (a) synthetic data; (b) numerical data; (c) measured data.

where $\|\mathbf{x}\| = \sqrt{\sum_{p=1}^{P}\sum_{q=1}^{Q}|x_{p,q}|^2}$, $\mathbf{E}^{\text{actual}}$ is the actual backscattered field, and $\mathbf{E}^{\text{recon}}$ is the reconstructed backscattered field by extracted scattering centers.

6. CONCLUSIONS

We proposed novel algorithms to extract one-dimensional and two-dimensional scattering centers. These algorithms can be fully operated automatically, are robust to noise, require no initial estimation, are not sensitive to model order, and can be computed quickly. Because the high resolution scattering center extraction algorithm is widely used in the field of radar signal processing, these algorithms are expected to be used in many applications. We especially expect that these algorithms will be used in radar target recognition, radar data compression, and denoising of radar receiving signals. The main idea of our proposed method can be used in other research fields such as extraction of complex natural resonance and scattering center extraction of synthetic aperture radar image [21, 22]. In future work, we will conduct research that applies the DROP algorithm to other areas.

ACKNOWLEDGMENT

This work was supported by the National Research Foundation of Korea (NRF) grant funded by the Korea government (MSIP; Ministry of Science, ICT & Future Planning) (No. NRF-2018R1D1A1B07041496).

REFERENCES

1. Shin, H., et al., "Analysis of radar cross section of a battleship equipped with an integrated mast module based on PO and PTD," *Journal of Electromagnetic Engineering and Science*, Vol. 17, No. 4, 238–240, Oct. 2017.
2. Kim, I. H., I. S. Choi, and D. Y. Chae, "A study on the performance enhancement of radar target classification using the two-level feature vector fusion method," *Journal of Electromagnetic Engineering and Science*, Vol. 18, No. 3, 206–211, Jul. 2018.
3. Hurst, M. and R. Mittra, "Scattering center analysis via Prony's method," *IEEE Transactions on Antennas and Propagation*, Vol. 35, No. 8, 986–988, Aug. 1987.
4. Pillai, S. U. and B. H. Kwon, "GEESE (GEneralized Eigenvalues Utilizing Signal Subspace Eignevectors) — A new technique for direction finding," *Twenty-second Asilomar Conference on Signals, Systems and Computers*, Vol. 2, 568–572, 1988.
5. Roy, R. and T. Kailath, "ESPRIT-estimation of signal parameters via rotational invariance techniques," *IEEE Transactions on Acoustics, Speech, and Signal Processing*, Vol. 37, No. 7, 984–995, Jul. 1989.
6. Hua, Y., "On SVD for estimating generalized eigenvalues of singular matrix pencil in noise," *IEEE Transactions on Signal Processing*, Vol. 39, No. 4, 9, 1991.
7. Hua, Y., "Estimating two-dimensional frequencies by matrix enhancement and matrix pencil," *IEEE Transactions on Signal Processing*, Vol. 40, 2267–2280, Sep. 1992.
8. Rouquette, S. and M. Najim, "Estimation of frequencies and damping factors by two-dimensional ESPRIT type methods," *IEEE Transactions on Signal Processing*, Vol. 49, No. 1, 9, 2001.
9. Quinquis, A., E. Radoi, and F.-C. Totir, "Some radar imagery results using superresolution techniques," *IEEE Transactions on Antennas and Propagation*, Vol. 52, No. 5, 1230–1244, May 2004.
10. Li, Q., E. J. Rothwell, K.-M. Chen, and D. P. Nyquist, "Scattering center analysis of radar targets using fitting scheme and genetic algorithm," *IEEE Transactions on Antennas and Propagation*, Vol. 44, No. 2, 198–207, Feb. 1996.
11. Choi, I. S. and H. T. Kim, "One-dimensional evolutionary programming-based CLEAN," *Electronics Letters*, Vol. 37, No. 6, 400–401, Mar. 2001.
12. Choi, I.-S. and H.-T. Kim, "Two-dimensional evolutionary programming-based CLEAN," *IEEE Transactions on Aerospace and Electronic Systems*, Vol. 39, No. 1, 373–382, Jan. 2003.
13. Choi, I.-S. and H.-T. Kim, "Generalized early-time/late-time evolutionary programming-based CLEAN," *Microwave and Optical Technology Letters*, Vol. 50, No. 1, 208–210, Jan. 2008.
14. Schwarz, U. J., "Mathematical-statistical description of the iterative beam removing technique (method CLEAN)," *Astron. Astrophy.*, Vol. 65, 345–356, 1978.
15. Choi, I.-S., "Performance comparison of PSO-based CLEAN and EP-based CLEAN for scattering center extraction," *Ubiquitous Computing and Multimedia Applications*, Vol. 150, 139–146, 2011.
16. Armijo, L., "Minimization of functions having Lipschitz continuous first partial derivatives," *Pacific Journal of Mathematics*, Vol. 16, No. 1, 1–3, Jan. 1966.
17. Choi, Y.-J. and I.-S. Choi, "A novel fast clean algorithm using the gradient descent method," *Microwave and Optical Technology Letters*, Vol. 59, No. 5, 1018–1022, May 2017.
18. Bydder, M., "Solution of a complex least squares problem with constrained phase," *Linear Algebra and Its Applications*, Vol. 433, 1719–1721, Dec. 2010.

19. Özdemir, C., *Inverse Synthetic Aperture Radar Imaging with MATLAB*, Wiley, Etobicoke, ON, Canada, 2012.
20. Cho, B.-L., I.-S. Choi, and E. J. Rothwell, "Enhanced ISAR imaging method using back-projection and SVA algorithm," *Microwave and Optical Technology Letters*, Vol. 57, No. 4, 993–997, 2015.
21. Rezaiesarlak, R. and M. Manteghi, "Complex-natural-resonance-based design of chipless RFID tag for high-density data," *IEEE Transactions on Antennas and Propagation*, Vol. 62, No. 2, 898–904, Feb. 2014.
22. Thirion-Lefevre, L. and E. Colin-Koeniguer, "Investigating attenuation, scattering phase center, and total height using simulated interferometric SAR images of forested areas," *IEEE Transactions on Geoscience and Remote Sensing*, Vol. 45, No. 10, 3172–3179, Oct. 2007.